electronics

MDPI

Article

Coordinated Reconfiguration with Energy Storage System for Load Restoration in Integrated Electric and Heating Systems

Ke Wang [1,2], Jing Wang [3,*], Pengfei Su [2] and Song Zhang [4]

[1] College of Electrical and Power Engineering, Taiyuan University of Technology, Taiyuan 030024, China; wangk50@cardiff.ac.uk
[2] School of Engineering, Cardiff University, Cardiff CF24 3AA, UK; sup2@cardiff.ac.uk
[3] Hebei Power Exchange Center, Shijiazhuang 050023, China
[4] School of Electrical Engineering, Northeast Electric Power University, Jilin 132012, China; zhangsong@neepu.edu.cn
* Correspondence: wjhz0621@126.com

Abstract: Coordinated load restoration of integrated electric and heating systems (IEHSs) has become indispensable following natural disasters due to the increasingly relevant integration between power distribution systems (PDS) and district heating systems (DHS). In this paper, a coordinated reconfiguration with an energy storage system is introduced to optimize load restoration in the aftermath of natural catastrophes. By modifying the DHS network topology, it is possible to maintain an uninterrupted energy supply in unfaulty zones by shifting heat loads among sources and adjusting the operation of coupled devices. Additionally, energy storage systems with rapid response times are implemented to enhance load restoration efficiency, especially when working in conjunction with multiple energy sources. Comprehensive case analyses have been systematically conducted to demonstrate the impact of coordinated reconfiguration with energy storage systems on improving load restoration.

Keywords: district heating system reconfiguration; energy storage system; integrated electric and heating system; load restoration

Citation: Wang, K.; Wang, J.; Su, P.; Zhang, S. Coordinated Reconfiguration with Energy Storage System for Load Restoration in Integrated Electric and Heating Systems. *Electronics* **2024**, *13*, 1931. https://doi.org/10.3390/electronics13101931

Academic Editor: Nikolay Hinov

Received: 1 April 2024
Revised: 8 May 2024
Accepted: 9 May 2024
Published: 15 May 2024

1. Introduction

In the last few years, frequent natural catastrophes have significantly impaired vast energy infrastructures, leading to widespread energy disruptions [1–3]. In 2021, Winter Storm Uri was a significant meteorological event that affected around 10 million people in Texas through the loss of their natural gas and electricity supply, with an estimated economic loss of up to USD 295 billion [4]. In 2022, Hurricane Ian damaged the power and natural gas transmission infrastructure in Florida, United States, affecting over 1.5 million individuals and resulting in economic losses of up to USD 67 billion [5].

With a growing consciousness of potential threats, the load restoration of integrated energy systems has increasingly come into focus [6,7]. The authors of [8] focused on the coordinated load restoration capabilities of district and regional integrated energy systems, aiming to bolster resilience following catastrophic events. The authors of [9] proposed a model for restoring electric and gas systems that incorporates coordination among subsystems. The authors of [10] proposed a restoration strategy considering the power distribution system reconfiguration and optimizing the deployment of repair crews.

The adoption of combined heat and power (CHP) units has established a closer relationship between electric and heating systems [11,12]. This connection has resulted in intricate interactions between the power distribution system (PDS) and the district heating system (DHS), posing two main issues. Firstly, there is the possibility of problem transmission from one system to the other through the coupled components, causing load shedding. For instance, improper switching operation in PDS might influence the heat

outputs of the CHP unit, resulting in the unnecessary shedding of heat loads [13]. Secondly, isolated subsystem operations can limit the potential to fully utilize the flexibility of the coupled components, such as CHP units, during the recovery phase. Thus, a collaborative approach is necessary for load restoration.

The reconfiguration of the DHS is a crucial step in the restoration of load in integrated electric and heating systems (IEHSs), analogous to the reconfiguration of PDSs [14]. DHSs can maintain a continuous heat supply in unaffected areas by shifting heat loads among sources and adjusting the network structure. This flexibility in managing heat distribution ensures that the system remains stable and efficient during disruptions. Furthermore, the DHS can enhance the effectiveness of restoration efforts by modifying the operational output of CHP units in coordination with PDS switch operations. This collaborative approach optimizes the recovery of both heat and power, thereby reducing the duration of outages and enhancing the ability of practitioners to respond to emergencies. Such strategic reconfiguration is of paramount importance in scenarios requiring rapid recovery from disruptions, such as severe weather conditions or other events that simultaneously impact power and heating infrastructures. The integration of heat and power restoration strategies serves to enhance the resilience of the IEHS against a range of disruptions, thereby facilitating a swift recovery and operational continuity.

Energy storage systems (ESSs) are becoming increasingly crucial for enhancing system recovery capabilities, particularly due to their rapid response speeds [15,16]. In the event of a system fault, the swift activation of energy storage systems (ESSs), combined with effective control strategies, plays a crucial role in maintaining the stability of power supply, particularly to critical loads. The instant compensatory capabilities of ESSs are pivotal in handling power disruptions. By seamlessly integrating ESSs with multiple energy sources, they ensure that no interruption occurs in the supply of power to essential services during outages. This integration is particularly critical in enhancing the resilience of integrated energy and heating systems (IEHSs) against natural disasters. ESSs facilitate a robust and flexible energy infrastructure that can quickly adapt to sudden changes in power availability. During disruptions caused by severe natural events, such as hurricanes or earthquakes, ESSs provide a reliable and continuous energy supply. This capability is essential for maintaining the operation of vital services like emergency response systems and other critical infrastructure. Moreover, the versatility of ESSs in integrating diverse energy sources enables a smooth transition between these sources during disruptions. This flexibility ensures that essential services remain operational, thereby mitigating the impact of the disaster on the community and economy. The strategic deployment of ESSs within IEHS frameworks significantly bolsters a system's ability to withstand and quickly recover from the catastrophic effects of natural disasters, providing a continuous and reliable energy supply during the most critical times.

This research puts forth a cooperative service-restoration model that incorporates the coordinated reconfiguration of subsystems and ESSs. The substantial contributions are summarized here, as follows:

(1) A model aiming to enable cooperative service restoration is introduced in this paper, accounting for the intricate interplay between the fault isolation and recovery phases. It highlights the fault propagation between the PDSs and DHSs and the collaborative recovery capability of subsystems in resisting natural disasters.
(2) Coordinated reconfiguration is provided to explore the flexibility of time-varying network topologies for service restoration. This strategy enhances the load restoration level by redistributing loads among different energy sources and fine-tuning the energy output of CHP units for improved energy provision.
(3) An energy storage system with fast response speeds is considered in restoration. which can ensure the continuation of power to vital loads. More importantly, the integration of energy storage systems with multiple energy sources can swiftly reinstate significant loads.

Section 2 provides a detailed introduction to the concept of IEHSs. Section 3 unveils a comprehensive model for fault recovery, highlighting the fault propagation and the importance of synchronized reconfiguration with ESS. The results on the P33H13 system and the study for future exploration are revealed in Section 4.

2. A Multi-Time Restoration Model

As shown in Figure 1, the power distribution system and the district heating system are synergistically linked in the IEHS, bridged by CHP units. As the main energy source for both PDSs and DHSs, CHP units significantly strengthen the interconnectivity and mutual support between these subsystems.

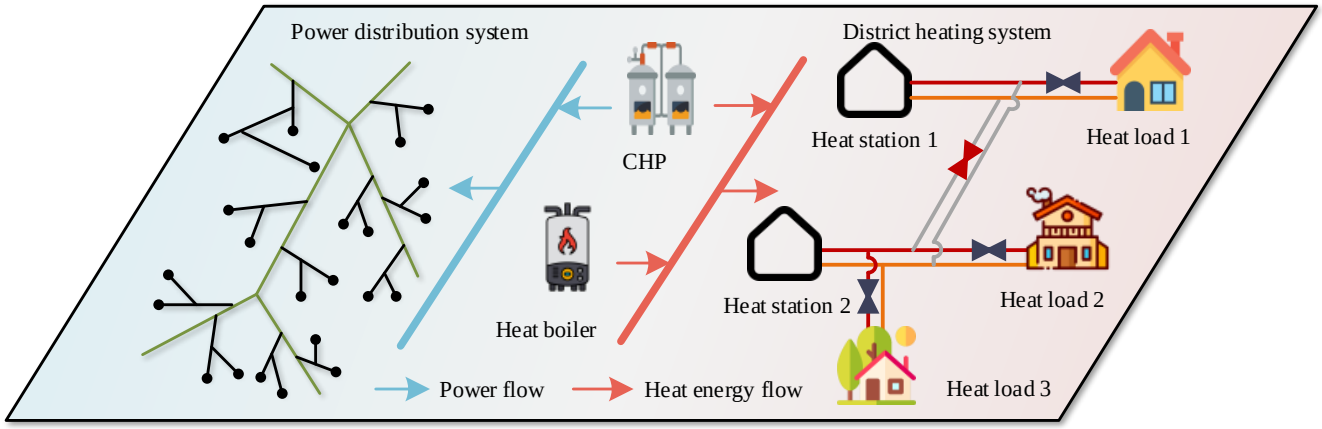

Figure 1. Structure of integrated electric and heating system.

As shown in Figure 2, an innovative collaborative model is specifically designed for service restoration, which integrates both fault isolation and subsequent restoration phases effectively. This model is especially pertinent when dealing with disruptions in complex energy systems like DHS and PDS.

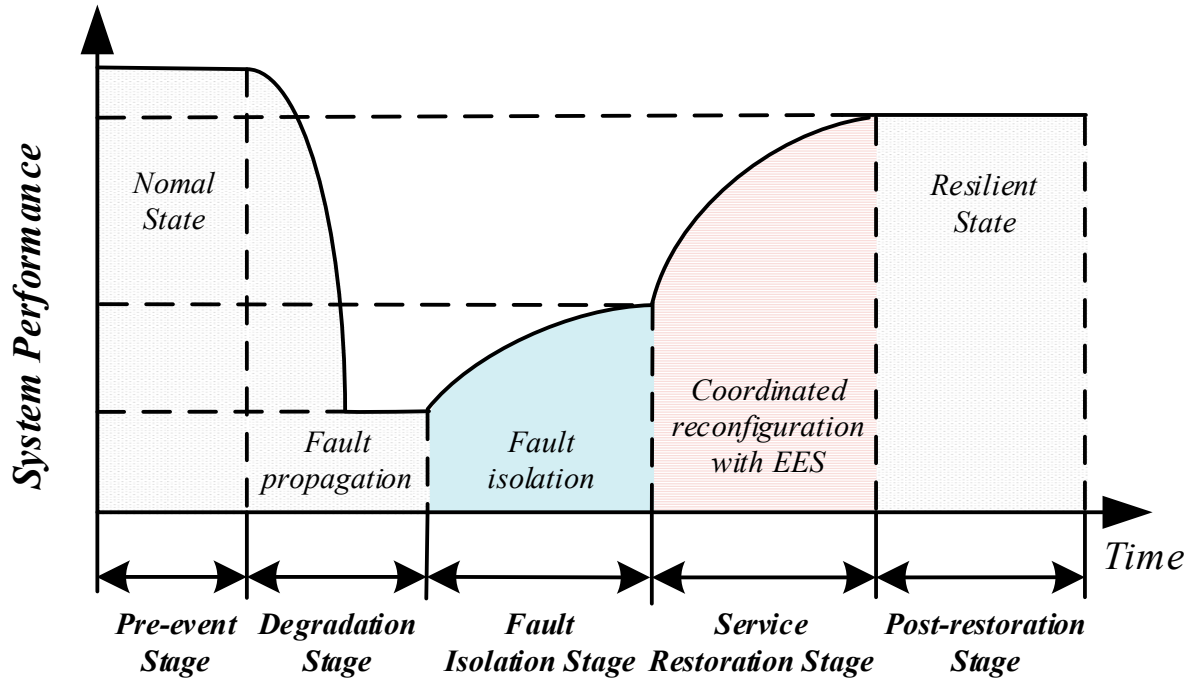

Figure 2. Resilience curve of an IEHS after disaster.

The initial phase, fault isolation, is crucial as it involves the joint operation of the DHS and PDS to pinpoint affected nodes or buses within the network. This operation helps in delineating the boundaries between fault and non-fault areas, which is essential for understanding and managing the scope of fault propagation effectively. By identifying these specific areas, the model facilitates targeted interventions, thereby optimizing the restoration process. Following fault isolation, the recovery phase commences. This phase is characterized by a coordinated reconfiguration of both the DHS and PDS. The objective here is to restore the services to the unaffected regions swiftly and efficiently, thus minimizing the downtime and impact on end users. This reconfiguration is complex, requiring precise control and synchronization between the heating and power sectors to ensure that loads in unaffected areas are restored without introducing new issues.

Moreover, the EES plays a pivotal role in the restoration process. EESs are utilized to maintain the continuity of the energy supply, particularly to vital loads that cannot withstand interruptions. These systems provide a buffer that helps in stabilizing the network during the restoration process by supplying stored energy when it is most needed. The model's effectiveness is further enhanced when integrated with multiple energy sources within an integrated energy and heating system (IEHS). By leveraging various energy sources, the EES can rapidly restore critical loads, thus ensuring that essential services remain operational during most of the restoration period. This integration not only improves the resilience of the system but also enhances its flexibility and responsiveness to disruptions.

2.1. Network Topological Constraints

2.1.1. Fault Isolation Model

In this stage, areas affected by faults show how faults propagate through the subsystem, which could give operators a detailed insight into the dynamics of the network during faults. It accurately delineates fault zones and traces fault propagation through the IEHS, as shown below:

$$\left(1-f_{ij}\right)\left(Y_{ij,0}-s_{ij,0}\right) \leq Y_{ij,t} \leq \left(1-f_{ij}\right)Y_{ij,0}, \forall (i,j) \in \mathbb{K}^p \cup \mathbb{K}^l, \forall t \in \mathbb{T}_i, \tag{1}$$

$$\mu_{j,t} - Y_{ij,0} + 1 \geq f_{ij}\left(1-s_{ij,0}\right), \forall (i,j) \in \mathbb{K}^p \cup \mathbb{K}^l, \forall t \in \mathbb{T}_i, \tag{2}$$

$$\mu_{j,t} - Y_{ij,0} + 1 \geq f_{ij}\left(1-s_{ij,0}\right), \forall (i,j) \in \mathbb{K}^p \cup \mathbb{K}^l, \forall t \in \mathbb{T}_i, \tag{3}$$

$$\mu_{j,t} - Y_{ij,t} + 1 \geq \mu_{j,t}, \forall (i,j) \in \mathbb{K}^p \cup \mathbb{K}^l, \forall t \in \mathbb{T}_i, \tag{4}$$

$$\mu_{j,t} - Y_{ij,t} + 1 \geq \mu_{j,t}, \forall (i,j) \in \mathbb{K}^p \cup \mathbb{K}^l, \forall t \in \mathbb{T}_i, \tag{5}$$

$$\mu_{m,t}^{CHP} = \mu_{s,t}^{CHP}, \forall m \in \mathbb{K}_{i,h}^{CHP}, h \in \mathbb{K}_{i,e}^{CHP}, \forall t \in \mathbb{T}_i, \tag{6}$$

Constraint (1) illustrates that the isolation process can be achieved by the switch/valve in an area that is not affected by faults. Constraints (2)–(3) indicate that if a pipe/line is not equipped with a switch/valve, the occurrence of a fault in it causes its connected nodes/buses to be classified as affected. Constraints (4)–(5) state that nodes/buses of a closed pipe/line are considered to be part of the same area. Constraint (6) specifies that any faults occurring in the CHP units within the DHS or PDS will be mirrored in the other subsystems. These constraints provide insight into the fault isolation dynamics of pipeline networks and establish a framework for prompts and precise fault detection.

2.1.2. Service-Restoration Model

After identifying the fault's exact location, the restoration strategy involves using switches and valves to restore the loads that were not isolated in the previous phase. This restoration procedure follows specific topological constraints.

$$\left(1-f_{ij,c}\right)\left(Y_{ij,t}-s_{ij,0}\right) \leq Y_{ij,t} \leq \left(1-f_{ij,c}\right)\left(Y_{ij,t}+s_{ij,0}\right), \forall (i,j) \in \mathbb{K}^p \cup \mathbb{K}^l, \forall t \in \mathbb{T}_r, \tag{7}$$

$$a_{ij,t} + a_{ji,t} = Y_{ij,t}, \forall (i,j) \in \mathbb{K}^p \cup \mathbb{K}^l, \forall t \in \mathbb{T}_r, \tag{8}$$

$$\sum_{i \in \pi(j)} a_{ij,t} \leq 1, \forall j \in \mathbb{K}^n, \forall t \in \mathbb{T}_r, \tag{9}$$

$$\sum_{s \in \sigma(j)} a_{js,t} = 0, \forall j \in \mathbb{K}^n, \forall t \in \mathbb{T}_r, \tag{10}$$

$$Y_{ij,t} = N_{ij} - N_s, \forall (i,j) \in \mathbb{K}^p \cup \mathbb{K}^l, \forall t \in \mathbb{T}_r, \tag{11}$$

$$\mu_{j,t} - Y_{ij,t} + 1 \geq \mu_{j,t}, \forall (i,j) \in \mathbb{K}^p \cup \mathbb{K}^l, \forall t \in \mathbb{T}_r, \tag{12}$$

$$\mu_{j,t} - Y_{ij,t} + 1 \geq \mu_{j,t}, \forall (i,j) \in \mathbb{K}^p \cup \mathbb{K}^l, \forall t \in \mathbb{T}_r, \tag{13}$$

Constraint (7) illustrates that switches/valves in non-faulted areas are crucial for the network's structural adjustment. Only the switch/valve equipped on the non-faulted pipe/line can be utilized for network reconfiguration. Constraints (8)–(10) illustrate that maintaining a radial network topology is essential in ensuring that energy flow follows a single route [17,18]. Constraints (12)–(13) illustrate that the nodes/buses of a closed pipe/line are considered to be part of the same area.

2.2. Operation Constraints

2.2.1. PDS Operation Constraints

A model for collaborative service restoration has been developed using mixed-integer second-order cone programming.

1. Power Balance Constraints

$$P_{j,t} = \sum_{s \in \delta(j)} P_{js,t} - \sum_{i \in \pi(j)} \left(P_{ij,t} - R_{ij} L_{ij,t}\right), \forall j \in \mathbb{K}^b, \forall t \in \mathbb{T}, \tag{14}$$

$$Q_{j,t} = \sum_{s \in \delta(j)} Q_{js,t} - \sum_{i \in \pi(j)} \left(Q_{ij,t} - X_{ij} L_{ij,t}\right), \forall j \in \mathbb{K}^b, \forall t \in \mathbb{T}, \tag{15}$$

$$P_{j,t} = P_{j,t}^{DG} + P_{j,t}^{CHP} + P_{j,t}^{EES} - \left(P_{j,t}^{L} - P_{j,t}^{Loss}\right), \forall j \in \mathbb{K}^b, \forall t \in \mathbb{T}, \tag{16}$$

$$Q_{j,t} = Q_{j,t}^{DG} + Q_{j,t}^{CHP} + Q_{j,t}^{EES} - \left(Q_{j,t}^{L} - Q_{j,t}^{Loss}\right), \forall j \in \mathbb{K}^b, \forall t \in \mathbb{T}, \tag{17}$$

$$\left\| 2P_{ij,t}\ 2Q_{ij,t}\ L_{ij,t} - U_{i,t} \right\|_2 \leq L_{ij,t} + U_{i,t}, \forall j \in \mathbb{K}^b, \forall t \in \mathbb{T}, \tag{18}$$

Constraints (14)–(17) illustrate the power flow at each bus. To improve the efficiency of the solution, the nonconvex current constraint is relaxed to a second-order cone constraint in (18). The treatment has been extensively used and justified in distribution systems [19,20].

2. Transmission Capacity Constraints

$$\left|P_{ij,t}\right| \leq Y_{ij,t} S_{ij}^{Max}, \forall (i,j) \in \mathbb{K}^l, \forall t \in \mathbb{T}, \tag{19}$$

$$\left|Q_{ij,t}\right| \leq Y_{ij,t} S_{ij}^{Max}, \forall (i,j) \in \mathbb{K}^l, \forall t \in \mathbb{T}, \tag{20}$$

Constraints (19)–(20) illustrate that the transmission power of a closed line should be within the bounds. The transmission power of an open line should be 0.

3. Voltage Drop Constraints

$$-\left(1 - Y_{ij,t}\right) M \leq U_{i,t} - U_{j,t} - 2\left(R_{ij} P_{ij,t} + X_{ij} Q_{ij,t}\right) + \left(R_{ij}^2 + X_{ij}^2\right) L_{ij,t} \leq \left(1 - Y_{ij,t}\right) M, \quad \forall (i,j) \in \mathbb{K}^l, \forall t \in \mathbb{T}, \tag{21}$$

$$U_j^{Min} \le U_{j,t} \le U_j^{Max}, \forall j \in \mathbb{K}^b, \forall t \in \mathbb{T}, \tag{22}$$

Constraint (21) illustrates that the voltage drops along a closed line. Constraint (22) illustrates that the voltage variation along the line should be within the bounds.

4. Unit Generation Constraints

$$(1-\mu_{j,t})P_{CHP,j}^{Min} \le P_{j,t}^{CHP} \le (1-\mu_{j,t})P_{CHP,j}^{Max}, \forall j \in \mathbb{K}^c, \forall t \in \mathbb{T}, \tag{23}$$

$$(1-\mu_{j,t})Q_{CHP,j}^{Min} \le Q_{j,t}^{CHP} \le (1-\mu_{j,t})Q_{CHP,j}^{Max}, \forall j \in \mathbb{K}^c, \forall t \in \mathbb{T}, \tag{24}$$

$$(1-\mu_{j,t})P_{DG,j}^{Min} \le P_{j,t}^{DG} \le (1-\mu_{j,t})P_{DG,j}^{Max}, \forall j \in \mathbb{K}^d, \forall t \in \mathbb{T}, \tag{25}$$

$$(1-\mu_{j,t})Q_{DG,j}^{Min} \le Q_{j,t}^{DG} \le (1-\mu_{j,t})Q_{DG,j}^{Max}, \forall j \in \mathbb{K}^d, \forall t \in \mathbb{T}, \tag{26}$$

Constraints (23)–(26) illustrate that the power generation of CHP units and DG should be within the bounds. When the power sources are cut off, the power generation is reduced to 0.

5. Load Shedding Constraints

$$\mu_{j,t}P_j^L \le P_{j,t}^{Loss} \le P_j^L, \forall j \in \mathbb{K}^d, \forall t \in \mathbb{T}, \tag{27}$$

$$\mu_{j,t}Q_j^L \le Q_{j,t}^{Loss} \le Q_j^L, \forall j \in \mathbb{K}^d, \forall t \in \mathbb{T}, \tag{28}$$

Constraints (27)–(28) demonstrate that, in faulted areas leading to unit shutdowns, electric loads will be completely removed, and in non-faulted areas, a portion of the loads will be shed to maintain power balance.

6. ESS Operation Constraints

$$E_{j,t}^{EES} = \begin{cases} E_{j,t-1}^{EES} - \frac{P_{j,t}^{EES} \cdot \Delta t}{\delta_j^{Dis}}, & if\ P_{j,t}^{EES} > 0 \\ E_{j,t-1}^{EES} - P_{j,t}^{EES} \cdot \Delta t \cdot \delta\delta_j^{Ch}, & if\ P_{j,t}^{EES} \le 0 \end{cases} \tag{29}$$

Constraint (29) demonstrates the dynamic limit of state for the energy stored in ESS and the charging/discharging power for two consecutive time slots, taking into account the charging/discharging efficiencies. It is important to specify the power flow direction of the ESS. When the value of $P_{j,t}^{EES}$ is positive, it indicates that the ESS is discharging, and when it is negative, it indicates that the ESS is charging.

$$SoC_{j,t} = \frac{E_{j,t}^{EES}}{E_j^{Cap.}}, \ \forall j \in \mathbb{K}^e, \forall t \in \mathbb{T}, \tag{30}$$

$$SoC_j^{Min} \le SoC_{j,t} \le SoC_j^{Max}, \ \forall j \in \mathbb{K}^e, \forall t \in \mathbb{T}, \tag{31}$$

Constraints (30)–(31) define the charge capacity boundaries for the ESS to prevent both excessive charging and discharging.

$$(1-\mu_{j,t})P_{EES,j}^{Min} \le P_{j,t}^{EES} \le (1-\mu_{j,t})P_{EES,j}^{Max}, \forall j \in \mathbb{K}^e, \forall t \in \mathbb{T}, \tag{32}$$

Constraint (32) illustrates the capacity limit of EES.

2.2.2. DHS Operation Constraints

In the energy flow model, the quantity of heat quantity is represented by an alternative variable, i.e., $H_{ij} = CM_{ij}\left(\tau_{ij}^{S} - \tau_{ij}^{R}\right)$, which is then incorporated into the service-restoration model [21–23].

1. Heat Station Constraints

$$\varsigma_j^{Min} H_{j,t}^{CHP} \le P_{j,t}^{CHP} \le \varsigma_j^{Max} H_{j,t}^{CHP}, \forall j \in \mathbb{K}^c, \forall t \in \mathbb{T}, \tag{33}$$

$$H_{j,t}^{HB} = \theta_j F_{j,t}^{HB}, \forall j \in \mathbb{K}^h, \forall t \in \mathbb{T}, \tag{34}$$

$$\sum_{j \in \mathbb{K}_i^c} H_{j,t}^{CHP} + \sum_{j \in \mathbb{K}_i^h} H_{j,t}^{HB} = H_{i,t}^{HS}, \forall i \in \mathbb{K}^{hs}, \forall t \in \mathbb{T}, \tag{35}$$

Constraint (33) illustrates the power-to-heat ratio of the CHP unit. Constraint (34) illustrates the ratio of fuel consumption to the production of a heating boiler (HB). Constraint (35) illustrates that heat generation in the heating station (HS) originates from the CHP unit and HB [24].

2. Heat Transmission Constraints

$$H_{ij,t}^{Out} = H_{ij,t}^{In} - H_{ij,t}^{Loss}, \forall (i,j) \in \mathbb{K}^p, \forall t \in \mathbb{T}, \tag{36}$$

$$\left|H_{ij,t}^{In}\right| \le Y_{ij,t} H_{ij}^{Max}, \forall (i,j) \in \mathbb{K}^p, \forall t \in \mathbb{T}, \tag{37}$$

$$\left|H_{ij,t}^{Out}\right| \le Y_{ij,t} H_{ij}^{Max}, \forall (i,j) \in \mathbb{K}^p, \forall t \in \mathbb{T}, \tag{38}$$

Constraint (36) illustrates the heat quantity loss from the inlet to the outlet pipe. Constraints (37)–(38) illustrate that the heat transmission along the pipe should be within the bounds. The heat transmission of an open line should be 0.

3. Energy Balance Constraints

$$\sum_{(j,s) \in S_j^{pipe-}} H_{js,t}^{Out} + \sum_{k \in \mathbb{K}_j^{HS}} H_{k,t}^{HS} = H_{j,t}^{L} - H_{j,t}^{Loss} + \sum_{(i,j) \in S_j^{pipe+}} H_{ij,t}^{In}, \forall j \in \mathbb{K}^n, \forall t \in \mathbb{T}, \tag{39}$$

Constraint (39) illustrates the heat flow at each node.

4. Unit Generation Constraints

$$(1 - \mu_{j,t}) H_{CHP,j}^{Min} \le H_{j,t}^{CHP} \le (1 - \mu_{j,t}) H_{CHP,j}^{Max}, \forall j \in \mathbb{K}^c, \forall t \in \mathbb{T}, \tag{40}$$

Constraint (40) illustrates that the heat generation of CHP units and HB should be within the bounds. When the heat sources are cut off, the heat generation is reduced to 0.

5. Load Shedding Constraints

$$\mu_{j,t} H_j^{L} \le H_{j,t}^{Loss} \le H_j^{L}, \forall j \in \mathbb{K}^n, \forall t \in \mathbb{T}, \tag{41}$$

Constraint (41) demonstrates that in regions affected by faults, heat loads will be completely shed, whereas areas without faults will experience partial load losses.

2.3. Objective and Resilience Metrics

The objective stated in (42) is to minimize the reduction in electrical and thermal loads during the fault restoration process. The resilience metric in (43) is to assess the level of load recovery with the proposed strategy.

$$\min \left\{ \Delta T_i \left(\sum_{j \in \mathbb{K}^b} \alpha_j P_{j,t}^{Loss} + \sum_{j \in \mathbb{K}^n} \beta_j H_{j,t}^{Loss} \right) + \Delta T_r \left(\sum_{j \in \mathbb{K}^n} \alpha_j P_{j,t}^{Loss} + \sum_{j \in \mathbb{K}^n} \beta_j H_{j,t}^{Loss} \right) \right\} + P_t^{Line}, \tag{42}$$

$$R_c = 1 - \frac{\Delta T_i \left(\sum_{j \in \mathbb{K}^b} \alpha_j P_{j,t}^{Loss} + \sum_{j \in \mathbb{K}^n} \beta_j H_{j,t}^{Loss} \right) + \Delta T_r \left(\sum_{j \in \mathbb{K}^b} \alpha_j P_{j,t}^{Loss} + \sum_{j \in \mathbb{K}^n} \beta_j H_{j,t}^{Loss} \right)}{(\Delta T_i + \Delta T_r) \left(\sum_{j \in \mathbb{K}^b} \alpha_j P_{j,t}^{L} + \sum_{j \in \mathbb{K}^n} \beta_j H_{j,t}^{L} \right)}. \tag{43}$$

3. Case Studies

3.1. Case Description

The proposed methodology is thoroughly tested using a specially adapted version of the P33H13 system, which is detailed in Figure 3. The modified 33-bus PDS is based on a standard IEEE 33-bus case, and the 14-node DHS is designed based on the 14-node DHS in [25] according to the design code of district heating network (CJJ34-2016). This system comprises three distinct heating stations, each equipped with advanced extraction condensing CHP units and a supplemental heating boiler. These installations are designed to efficiently meet the heating demands of the system.

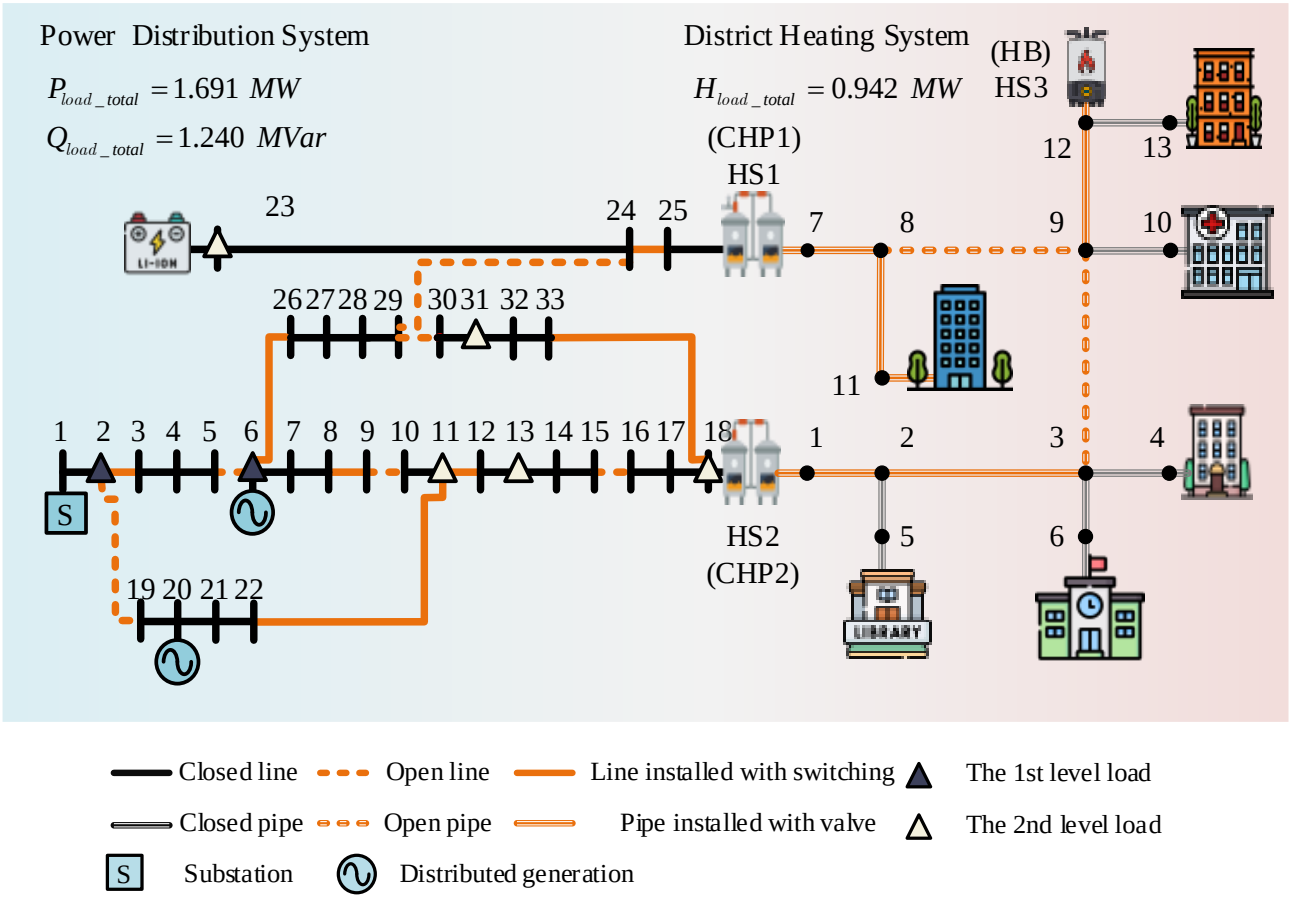

Figure 3. Structure of P33H13 system.

Prior to any significant events, particular operational setups are made—specifically, certain valves and switches are strategically left open. This configuration is critical as it allows for a seamless transition and flexibility in operations during routine functions or in the event of system adjustments. Moreover, the IEHS incorporated within the setup includes small-scale CHP units. These micro-gas turbines play a pivotal role as they link

the park-level heating system with the distribution power system, thereby enhancing the system's integration and operational efficiency.

Figure 3 provides a clear visual representation of the connections and layout of these components, emphasizing the synergy between the park-level heating and power distribution systems. This integration is essential for optimizing the energy flow and ensuring stability across both networks. The system's capacity to handle electrical and heat loads was rigorously evaluated. The total electric and reactive power loads of the system are recorded at 1.691 MW and 1.240 MVar, respectively, while the thermal load is approximately 0.942 MW. Both the DG and CHP units possess a capacity of 0.5 MVA and 0.5 MW, respectively, illustrating a well-balanced distribution of power and heating capabilities across the system. The experiments are carried out on a computer equipped with an i7-1165G7 CPU and 16 GB of memory, which is programmed by Matlab R2020a.

3.2. Case Analysis

To illustrate the effect of synchronized reconfiguration with EES, three cases are examined:

Case 1: Load restoration only by network reconfiguration in PDS.

Case 2: Load restoration considering coordinated network reconfiguration.

Case 3: Load restoration incorporating both the coordinated reconfiguration strategy and the utilization of an energy storage system.

3.2.1. PDS Fault Scenario

In this scenario, lines LB6-26, LB8-9, LB11-12, and LB23-24 suffered destruction due to natural catastrophes. This led to significant power and heating disruptions across the IEHS. The effects of these incidents are detailed in Table 1, from which conclusions can be inferred.

Table 1. Load restoration and resilience metrics.

Scenario	Case	Complete Load Restoration (MW)	Load Restoration (MW)		Resilience Metrics
			Electric Load	Heat Load	
PDS	Case 1	29.65	22.33	7.32	0.78
	Case 2	35.79	22.63	13.16	0.85
	Case 3	36.51	23.35	13.16	0.88
DHS	Case 1	25.11	17.85	7.26	0.73
	Case 2	28.85	18.21	10.64	0.76
	Case 3	30.24	19.2	11.04	0.80

The initial interference with line LB23-24 in the PDS had repercussions in the DHS, mediated by the CHP units, which led to restricted output from CHP1 during the fault isolation stage. This resulted in the total loss of the second-level electric load at bus 23 and the partial diminishment of heat loads at nodes 8 and 11.

Secondly, a coordinated reconfiguration is carried out, which involves the remote orchestration of valves/switches and the equitable distribution of loads across multiple energy sources. In Case 2, valves implemented on pipes PN3-9, PN7-8, and PN8-9 redistribute the heat loads of the CHP2 unit, reducing the amount of load shedding within the DHS.

Thirdly, energy storage systems can provide quick backup electricity to ensure the continuous operation of critical facilities and services. In Case 3, the switch implemented on lines LB24-29 transfers the electric loads at buses 23, 24, 26, 27, 28, and 29 to the energy storage system, reducing the amount of load shedding within the PDS.

As shown in Figure 4, as the application of energy storage and grid reconfiguration strategies is implemented, there is a gradual increase in the amount of load recovery observed. The needed time for restoration and fault clearance in Cases 2 and 3 are 10 min and 7 min. These technologies enhance the system's capacity to rapidly adapt and restore power and heat loads following disruptions, thereby ensuring a more resilient and efficient energy

supply. The progressive deployment of storage and restructuring measures effectively mitigates the impact of outages, leading to improved stability and reduced restoration time in energy networks.

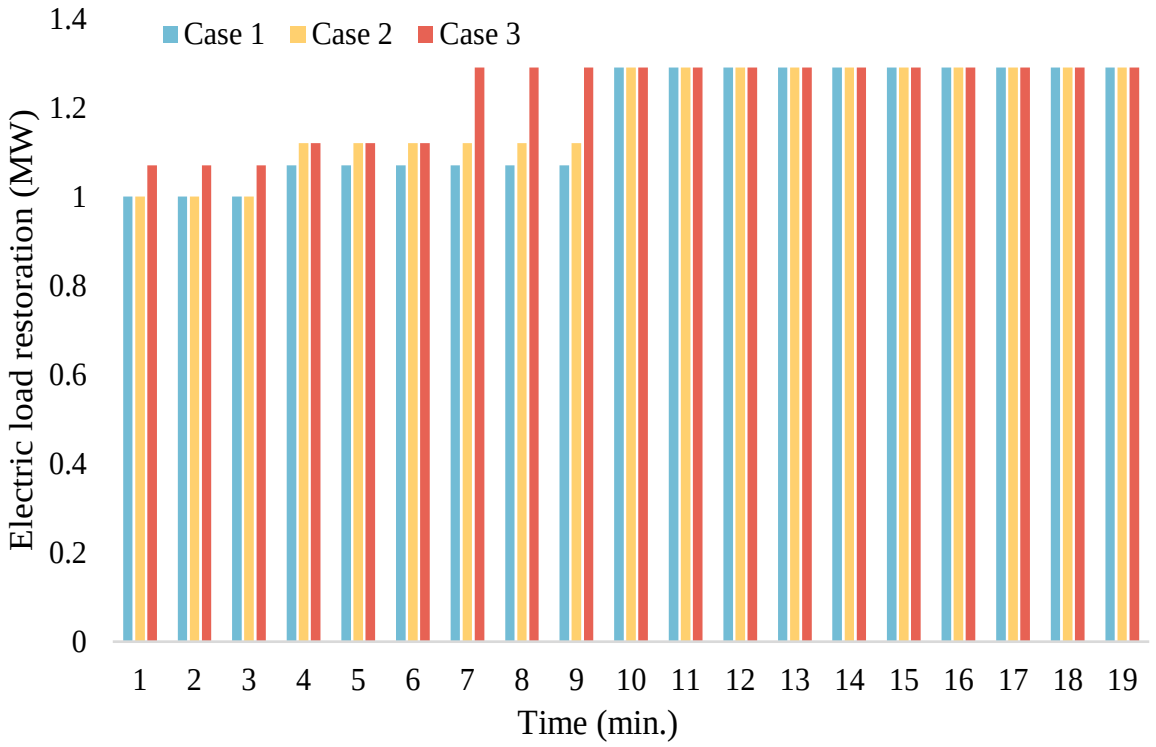

(**a**)

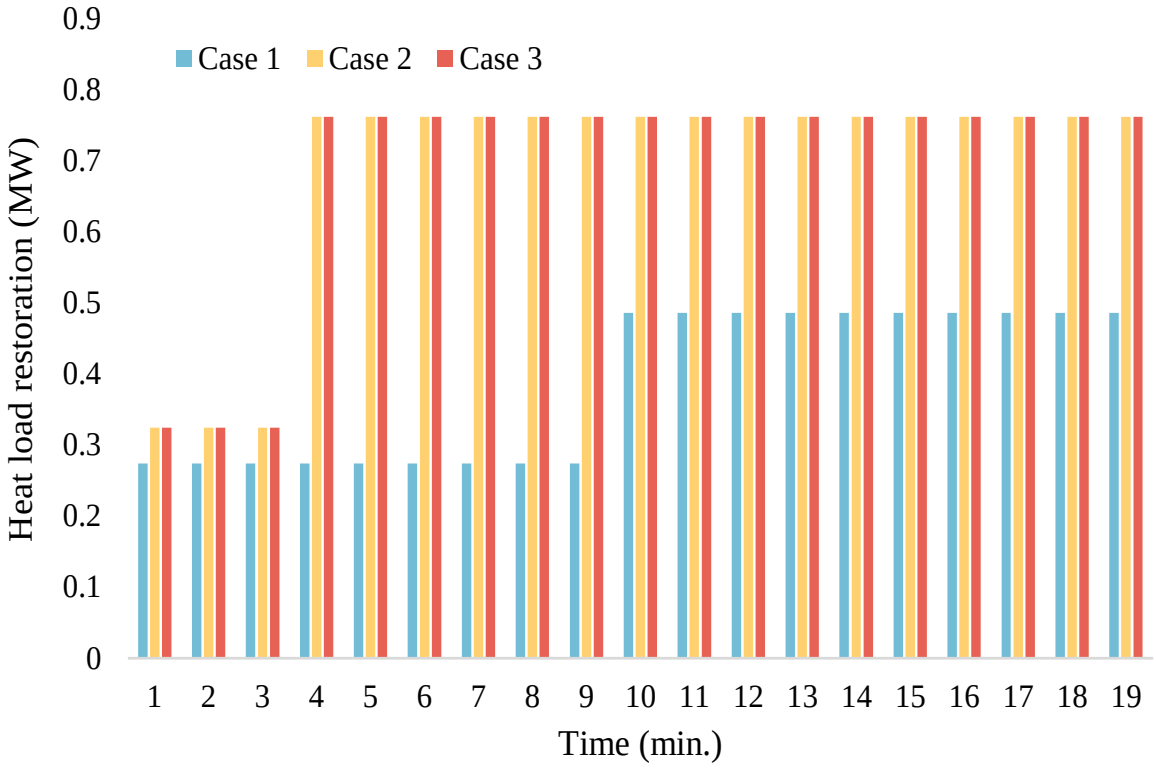

(**b**)

Figure 4. Load restoration. (**a**) Electric loas restoration. (**b**) Heat loas restoration.

3.2.2. DHS Fault Scenario

Table 1 elucidates the sequence of switch and valve operations after disasters affected pipes PN2-3, PN2-11, and PN12-13. Table 1 provides a comprehensive illustration of the total load recovery amounts under distinct fault scenarios and cases, with a particular focus on the electrical and thermal load shedding quantities. Furthermore, the table includes resilience metrics that quantify the effectiveness of the system in withstanding and recovering from these disturbances. By comparing the resilience indicators across different cases, the table offers a comprehensive overview of the system resilience in maintaining functionality during and after faults. This allows for an in-depth analysis of the effectiveness of implemented measures.

Firstly, the occurrence of a disruption in pipe PN2-3 within the DHS leads to significant interruptions in both power and heat supply. This disruption directly affects the heat loads at nodes 3, 4, and 6, which in turn causes a noticeable decrease in electrical loads at buses 30 and 31. The primary reason for this decrease is the diminished energy production capacity of the CHP2. Such reductions in energy output necessitate immediate adjustments to prevent extensive service downtimes.

To address these challenges and enhance the resilience of the system, adjustments to the configuration of the district heating network are essential. One effective strategy is the redistribution of heat loads, particularly in response to disaster scenarios. For instance, in Case 2, the heat loads at nodes 3, 4, and 6 are efficiently redistributed. This is achieved through strategic valve operations within the network, specifically in pipes PN3-9, PN8-9, and PN9-12. By manipulating the flow through these critical junctions, it is possible to improve overall energy distribution.

Furthermore, such adjustments contribute significantly to the operational flexibility of the CHP1. This flexibility is crucial for the quick restoration of system load, especially in times of unexpected failures or maintenance activities. The enhanced flexibility not only helps in managing the immediate effects of the disruption but also prepares the network for future contingencies by improving its adaptive capabilities.

Thirdly, the implementation of ESS stands out as a key measure to provide rapid backup power and ensure the uninterrupted functioning of essential facilities and services. In Case 3, the operationalization of a switching mechanism along the LB24-29 lines effectively channels the electrical loads of buses 23, 24, 26, 27, 28, and 29 toward an energy storage system. This strategic maneuver significantly reduces load shedding within the PDS.

3.2.3. Discussion

A coordinated reconfiguration strategy with EES is more effective for load restoration in IEHS. Under the PDS fault scenario, there is a significant increase in load restoration (2.0%, 23.1%) and a notable enhancement in the resilience metric (3.5%, 12.8%) in Case 3 compared to Cases 1 and 2. Under the DHS fault scenario, a comparative analysis reveals a significant increase in load restoration (4.8% 20.4%) and a significant improvement in the resilience metric (5.3%, 9.6%) in Case 3 when compared to the results of Cases 1 and 2.

4. Conclusions

In this study, we introduce a strategy for service restoration that effectively combines network reconfiguration and EES within IEHS. This method meticulously considers the dynamic interactions between fault isolation and service restoration phases, elucidating the complex dependency between PDS and DHS. The main conclusions are summarized here, as follows: (i) the disturbances within the PDS significantly influence the DHS operations via interconnected elements; (ii) the strategic adjustments in DHS configurations to enable them to cooperate with PDS reconfiguration can enhance the flexibility of energy distribution, by effectively reallocating loads among various energy sources; (iii) the EES can mitigate the effects of load reductions during cross-system disturbances. By precisely adjusting the output of EES, we have significantly enhanced the resilience of IEHS, quan-

tifiably improving energy efficiency and system reliability under stress conditions. This targeted approach ensures a more robust and responsive infrastructure, leading to an average resilience improvement of 10.32% across tested scenarios.

Moving forward, we aim to delve into a broader spectrum of uncertainties, including variability in demand and unexpected system failures. Fundamentally, our research underscores the critical role of coordinated network reconfiguration in fortifying the robustness of IEHSs and offers valuable directions for forthcoming investigations in this field. Also, a further study for service restoration considering the time scales between PDSs and DHSs, the economic costs of switch/valve operations, and the utilization of energy storage systems will be performed and reported in the future.

Author Contributions: Writing—original draft, K.W.; Writing—review & editing, J.W., P.S. and S.Z. All authors have read and agreed to the published version of the manuscript.

Funding: This research received no external funding.

Data Availability Statement: Data are contained within the article.

Conflicts of Interest: The authors declare no conflict of interest.

Nomenclature

A	*Indices and Sets*
t	Index of time
$\mathbb{T}_i$	Index of fault isolation phase
$\mathbb{T}_r$	Index of load restoration phase
$\mathbb{K}_i^{CHP}$	Set of CHP units installed in heat station i
$\mathbb{K}^p/\mathbb{K}^l$	Set of transmission lines and heating pipes
$\mathbb{K}^b/\mathbb{K}^n$	Set of PDS buses and DHS nodes
$\mathbb{K}^c$	Set of CHP units
$\mathbb{K}^h$	Set of heating boilers
$\mathbb{K}^{hs}$	Set of heating exchange stations
$k_j^{pipe,\text{in}}/k_j^{pipe,out}$	Set of pipes originating from/leading to node j
B	*Parameters*
$Y_{ij,0}$	Boolean variable reflecting the operational/non-operational status of line/pipe (i,j) in normal condition
$s_{ij,0}$	Boolean variable, the valve/switch on pipe/line (i,j) is engaged and open when $s_{ij,0}=1$, the pipe/line does not contain any switch/valve or it is in a closed state when $s_{ij,0}=0$
f_{ij}	Boolean variable that represents if line/pipe (i,j) has incurred damage due to a catastrophic event.
n_s	Quantity of nodes/buses
n_{ij}	Quantity of transmission lines/heating pipes
R_{ij}/X_{ij}	Resistance and reactance of line (i,j)
S_{ij}^{Max}	Maximum transmission capability of line (i,j)
U_j^{Min}/U_j^{Max}	Range of squared voltage magnitudes from minimum to maximum the bus j
$P_{DG,j}^{Min}/P_{DG,j}^{Max}$	Range of power output of distributed generation j
$P_{CHP,j}^{Min}/P_{CHP,j}^{Max}$	Range of power output of CHP unit j
$P_{EES,j}^{Min}/P_{EES,j}^{Max}$	Range of power output of EES j from minimum to maximum
Δt	Time interval
$\delta_j^{Dis}/\delta_j^{Ch}$	Charging/discharging efficiency of ESS j
$E_j^{Cap.}$	Capacity of ESS j

SoC_j^{Min}/SoC_j^{Max}	Range of state of charge of ESS j
$\varsigma_j^{Min}/\varsigma_j^{Max}$	Range of power to heat ratio of CHP unit j from minimum to maximum
θ_j	Proportion of fuel consumption to heat generation of HB j
H_{ij}^{Max}	Transmission capability of heat quantity of pipe (i,j)
α_j/β_j	Weight factor of electric and heat load j
$\Delta T_i/\Delta T_r$	Fault isolation and load restoration duration
C	*Variables*
$Y_{ij,t}$	Boolean variable reflecting the operational/non-operational status of line/pipe (i,j) at t
$\mu_{j,t}$	Boolean variable that illustrates the status of a bus/node i as either functioning or malfunctioning.
$L_{ij,t}$	Current magnitude squared of line (i,j) at t
$P_{j,t}/Q_{j,t}$	Power infusion of bus i at t
$P_{js,t}/Q_{js,t}$	Power flow from bus j to bus s at t
$P_{j,t}^{DG}/Q_{j,t}^{DG}$	Power output of distributed generation j at t
$P_{j,t}^{CHP}/Q_{j,t}^{CHP}$	Power output of CHP unit j at t
$P_{j,t}^{EES}/Q_{j,t}^{EES}$	Charging/discharging power of EES j at t
$E_{j,t}^{EES}$	Energy stored in ESS at t
$P_{j,t}^{L}/Q_{j,t}^{L}$	Electrical load of bus j at t
$P_{j,t}^{Loss}/Q_{j,t}^{Loss}$	Decrease in electrical load of bus j at t
$U_{i,t}$	Squared voltage magnitude of bus j at t
$H_{j,t}^{CHP}$	Heat output of CHP unit j at t
$H_{j,t}^{HB}$	Heat output of heating boiler j at t
$F_{j,t}^{HB}$	Amount of fuel expended by the heating boiler j at t
$H_{k,t}^{HS}$	Heat output of heat station k at t
$H_{ij,t}^{In}/H_{ij,t}^{Out}$	Thermal energy flow into and out of the pipeline (i,j) at t
$H_{ij,t}^{Loss}$	Heat quantity reduction within the pipe (i,j) at t
$H_{j,t}^{Loss}$	Heat quantity reduction of node j at t
P_t^{Line}	Power losses in transmission of line (i,j) at t

References

1. Wang, C.; Wei, W.; Wang, J.; Liu, F.; Qiu, F.; Correa-Posada, C.M.; Mei, S. Robust Defense Strategy for Gas–Electric Systems Against Malicious Attacks. *IEEE Trans. Power Syst.* **2017**, *32*, 2953–2965. [CrossRef]
2. Amirioun, M.H.; Aminifar, F.; Shahidehpour, M. Resilience-Promoting Proactive Scheduling Against Hurricanes in Multiple Energy Carrier Microgrids. *IEEE Trans. Power Syst.* **2019**, *34*, 2160–2168. [CrossRef]
3. Wang, K.; Xue, Y.; Guo, Q.; Shahidehpour, M.; Zhou, Q.; Wang, B.; Sun, H. A Coordinated Reconfiguration Strategy for Multi-Stage Resilience Enhancement in Integrated Power Distribution and Heating Networks. *IEEE Trans. Smart Grid* **2023**, *14*, 2709–2722. [CrossRef]
4. Nejat, A.; Solitare, L.; Pettitt, E.; Mohsenian-Rad, H. Equitable Community Resilience: The Case of Winter Storm Uri in Texas. *Int. J. Disaster Risk Reduct.* **2022**, *77*, 103070. [CrossRef]
5. Hurricane Ian after-Action Report. Available online: https://ahca.myflorida.com/content/download/23000/file/After%20Action%20Report%20Hurricane%20Ian.pdf (accessed on 1 August 2023).
6. Manshadi, S.D.; Khodayar, M.E. Resilient Operation of Multiple Energy Carrier Microgrids. *IEEE Trans. Smart Grid* **2015**, *6*, 2283–2292. [CrossRef]
7. Zheng, W.; Lu, H.; Zhang, M.; Wu, Q.; Hou, Y.; Zhu, J. Distributed Energy Management of Multi-entity Integrated Electricity and Heat Systems: A Review of Architectures, Optimization Algorithms, and Prospects. *IEEE Trans. Smart Grid* **2024**, *15*, 1544–1561. [CrossRef]
8. Yan, M.; He, Y.; Shahidehpour, M.; Ai, X.; Li, Z.; Wen, J. Coordinated Regional-District Operation of Integrated Energy Systems for Resilience Enhancement in Natural Disasters. *IEEE Trans. Smart Grid* **2019**, *10*, 4881–4892. [CrossRef]
9. Li, G.; Yan, K.; Zhang, R.; Jiang, T.; Li, X.; Chen, H. Resilience-Oriented Distributed Load Restoration Method for Integrated Power Distribution and Natural Gas Systems. *IEEE Trans. Sustain. Energy* **2022**, *13*, 341–352. [CrossRef]
10. Lin, Y.; Chen, B.; Wang, J.; Bie, Z. A Combined Repair Crew Dispatch Problem for Resilient Electric and Natural Gas System Considering Reconfiguration and DG Islanding. *IEEE Trans. Power Syst.* **2019**, *34*, 2755–2767. [CrossRef]
11. Pan, Z.; Guo, Q.; Sun, H. Feasible Region Method Based Integrated Heat and Electricity Dispatch Considering Building Thermal Inertia. *Appl. Energy* **2017**, *192*, 395–407. [CrossRef]

12. Wang, Y.; Xu, Y.; He, J.; Liu, C.-C.; Schneider, K.P.; Hong, M.; Ton, D.T. Coordinating Multiple Sources for Service Restoration to Enhance Resilience of Distribution Systems. *IEEE Trans. Smart Grid* **2019**, *10*, 5781–5793. [CrossRef]
13. Khatibi, M.; Bendtsen, J.D.; Stoustrup, J.; Molbak, T. Exploiting Power-to-Heat Assets in District Heating Networks to Regulate Electric Power Network. *IEEE Trans. Smart Grid* **2021**, *12*, 2048–2059. [CrossRef]
14. Mao, D.; Wang, P.; Wang, W.; Ni, L. Reliability Segment Design in Single-Source District Heating Networks Based on Valve Network Models. *Sustain. Cities Soc.* **2020**, *63*, 102463. [CrossRef]
15. Akaber, P.; Moussa, B.; Debbabi, M.; Assi, C. Automated Post-Failure Service Restoration in Smart Grid Through Network Reconfiguration in the Presence of Energy Storage Systems. *IEEE Syst. J.* **2019**, *13*, 3358–3367. [CrossRef]
16. Yin, H.; Wang, Z.; Liu, Y.; Qudaih, Y.; Tang, D.; Liu, J.; Liu, T. Operational Reliability Assessment of Distribution Network With Energy Storage Systems. *IEEE Syst. J.* **2023**, *17*, 629–639. [CrossRef]
17. Lei, S.; Chen, C.; Song, Y.; Hou, Y. Radiality constraints for resilient reconfiguration of distribution systems: Formulation and application to microgrid formation. *IEEE Trans. Smart Grid* **2020**, *9*, 3944–3956. [CrossRef]
18. Lei, S.; Wang, J.; Hou, Y. Remote-controlled switch allocation enabling prompt restoration of distribution systems. *IEEE Trans. Power Syst.* **2018**, *5*, 3129–3142. [CrossRef]
19. Arif, A.; Cui, B.; Wang, Z. Switching Device-Cognizant Sequential Distribution System Restoration. *IEEE Trans. Power Syst.* **2022**, *1*, 317–329. [CrossRef]
20. Li, Z.; Su, S.; Jin, X.; Xia, M.; Chen, Q.; Yamashita, K. Stochastic and Distributed Optimal Energy Management of Active Distribution Networks Within Integrated Office Buildings. *CSEE J. Power Energy Syst.* **2024**, *10*, 504–517.
21. Li, Z.; Xu, Y.; Wang, P.; Xiao, G. Coordinated preparation and recovery of a post-disaster Multi-energy distribution system considering thermal inertia and diverse uncertainties. *Appl. Energy* **2023**, *336*, 120736. [CrossRef]
22. Ding, B.; Li, Z.; Li, Z.; Xue, Y.; Chang, X.; Su, J.; Jin, X.; Sun, H. A CCP-based distributed cooperative operation strategy for multi-agent energy systems integrated with wind, solar, and buildings. *Appl. Energy* **2024**, *365*, 123275. [CrossRef]
23. Ding, Y.; Shao, C.; Hu, B.; Bao, M.; Niu, T.; Xie, K.; Singh, C. Operational Reliability Assessment of Integrated Heat and Electricity Systems Considering the Load Uncertainties. *IEEE Trans. Smart Grid* **2021**, *12*, 3928–3939. [CrossRef]
24. Sarantakos, I.; Zografou-Barredo, N.-M.; Huo, D.; Greenwood, D. A Reliability-Based Method to Quantify the Capacity Value of Soft Open Points in Distribution Networks. *IEEE Trans. Power Syst.* **2021**, *36*, 5032–5043. [CrossRef]
25. Wang, K.; Xue, Y.; Zhou, Y.; Zening, L.; Xinyue, C.; Sun, H. Distributed coordinated reconfiguration with soft open points for resilience-oriented restoration in integrated electric and heating systems. *Appl. Energy* **2024**, *365*, 123207. [CrossRef]